

CHAPTER THREE

CLASSIFICATION OF STRUCTURES LEFT BY MICROBIAL MATS IN THEIR HOST SEDIMENTS

**P.G. Eriksson, J. Schieber, E. Bouougri, G. Gerdes, H. Porada,
S. Banerjee, P.K. Bose and S. Sarkar**

Introduction

We view the structures and features described in this atlas as sedimentary structures, albeit of a complex organo-physico-chemical origin. Just like their physical sedimentary structure counterparts (e.g., Pettijohn and Potter, 1964), they can be of great assistance in unravelling depositional palaeoenvironments inferred for ancient rock successions. Pettijohn and Potter (1964) included stromatolites in their well known classification of primary physical sedimentary structures, under their class 2E structures, as positive growth features upon bedding planes (Noffke et al., 2001a). The combination of microbial construction, accretion of detrital grains, and biochemical precipitation implicit in stromatolite formation (e.g., Walter, 1976) was originally thought to be endemic to carbonate-forming settings (e.g., Awramik, 1984; Walter et al., 1992; Altermann, 2004). There is a growing recognition, however, that surficial microbial communities interacted with physical agents of erosion, sedimentation and even deformation (Noffke et al., 2001a) in ancient clastic sedimentary settings (e.g., Schieber, 1986, 1998a, 1999, 2004; Hagadorn et al., 1999; Gehling, 1999; Pflüger, 1999). A large array of modern examples of resultant features, both microbial and clastic-sedimentary has been presented in Chapter 2 of this book.

Classification of stromatolites has a long and contentious history (see recent summary in Altermann, 2004), with the best result likely having been achieved by Hofmann (1973, updated 2000). Hofmann proposed a pyramidal diagram, in which each of the four corners represented one of the four main genetic processes, namely biological non-skeletal, biological skeletal, mechanical clastic, and chemical. Classification of the infinitely more complex set of microbial mat features preserved in sandstones and mudrocks, as presented in this atlas, is a much more challenging task. As for carbonates, genetically-based approaches seem to enjoy the broadest acceptance.

Three main genetic classification schemes have appeared in recent years. Gerdes et al. (2000a) examined modern textural signatures of microbial activity in two chosen study

areas of siliciclastic sediments along the peritidal coastlines of the North Sea and Tunisia. They recognised six types of biogenically mediated clastic sedimentary fabrics, those due to:

- (1) intrinsic biofactors – i.e., essentially the morphology and behaviour of biofilms and their more robust counterparts, microbial mats;
- (2) biological response to physical disturbances;
- (3) trapping and binding of clastic sediment;
- (4) mechanical deformation of biologically stabilised clastic sediment surfaces;
- (5) post-burial processes;
- (6) bioturbation processes.

Although Gerdes et al. (2000a) clearly recognised that this scheme was a catalogue of microbial signatures in modern peritidal clastic settings, the potential fossilisation of these fabrics/features meant that it also could provide the basis for a genetic classification scheme. This same team of authors, with the addition of Krumbein (Noffke et al., 2001a) published a formal classification scheme for what they termed ‘microbially-induced sedimentary structures’ (MISS), arguing logically in favour of these forming a fifth category in the well-known Pettijohn and Potter (1964) classification scheme for primary (physical) sedimentary structures. Once again, this was a scheme based on genetic factors. Noffke et al. (2001a) proposed two classes of MISS: (class A) structures atop bedding planes, and (class B) those within beds:

- (1) class A: (a) levelled depositional surfaces and wrinkle marks;
(b) microbial mat chips;
(c) erosional remnants and pockets;
(d) multidirectional or palimpsest ripples;
(e) mat curls, shrinkage cracks.
- (2) class B: (a) sponge pore fabrics, gas domes, fenestrae structures;
(b) sinoidal laminae;
(c) oriented grains, benthic ooids;
(d) biolaminites, mat-layer-bound grain sizes.

The third classification scheme for microbial mat features preserved in the siliciclastic rock record is that of Schieber (2004), who emphasized that microbial mats influence the depositional fabric of clastic deposits across a wide range of physical, chemical and biological processes. He further stressed that these mat-related structures and features are in many ways analogous to trace fossils, and that the influence and thus former presence of mats can be inferred from observations suggesting sediment properties that would be uncharacteristic for a purely physically deposited sand or mud. Useful features are those that indicate original sediment cohesiveness, tensile strength, and erosion-resistance during deposition, and those that allow deduction of original permeability and geochemical behaviour during early diagenesis. His classification scheme encompassed a set of features that spans the process continuum from active mat growth, through mat metabolism, and on to mat destruction, and finally, mat decay and diagenesis (Figs. 3-1

and 3-2). He presented separate, yet basically analogous schemes for mat-related features from sandstones and mudrocks (Figs. 7.9-1 and 7.9-2 in Schieber, 2004). Schieber (op. cit.) also stressed that several of the observed features could have multiple origins (e.g., ‘*Astropolithon*’ gas or fluid escape structures in Chapter 4(a) and (d), or ripple patches in Chapter 4(a) and (c)), something already implicit if not always fully apparent, from earlier classification schemes. This scheme is discussed in some detail below as it is the classification followed in this book. Some minor adaptations have been made to this published scheme here, and an additional short section illustrating complex structures resulting from microbial mats has been added.

Schieber’s (2004) classification

Microbial mat features preserved in sandstones (see Chapter 4)

Figure 3-1 summarises features that have been observed in sandstones subject to microbial mat influences during deposition or diagenesis. Genetic processes inferred to be responsible for these biogenic sedimentary structures are shown on a clockwise-arranged continuum, from mat growth to final destruction and diagenesis (cf. Schieber, 2004).

Features formed under conditions of mat growth (see Chapter 4(a))

Biostabilisation of clastic sediment (cf. Gerdes et al., 2000a) encompasses binding, trapping, and baffling. Thin biofilms comprising intermingled sand grains and microbial filaments tend to stabilise sediment surfaces following physical reworking processes. Any surface morphology from such sediment layers can then be ‘frozen’; **multiple-directed ripple marks** (Noffke, 1998a) may form during further reworking, or, if new sediment is introduced (Pflüger, 1999), **palimpsest ripples** (‘a’ in Fig. 3-1) may develop. If reworking has sufficient energy, ripple crests may partially be removed, with **narrow ridges** (‘b’, Fig. 3-1; see also cracked and eroded ripple crests in Figs. 4(a)-17 and -18) surviving to attest to erosion-resistance provided by mat growth and concomitant cohesion (Pflüger, 1999). As with many mat features, those described in this paragraph also reflect a combination of factors. Some physical modification, or even partial destruction, is inherent apart from the initial mat growth influences. Pliable spheroidal sand clasts, reflecting non-sorted, sticky sand clasts which deform each other, are an additional feature to those detailed by Schieber (2004) and are illustrated in Figs. 4(a)-3 and -4.

Analogous binding and trapping of sediment grains can also result in characteristic laminar features. These comprise evidence for microbial mats preserved in single laminae as well as in biolaminated deposits (cf. biolaminites). In some modern environments, laminae of **horizontally oriented mineral grains** alternate with graded laminae (‘c’, Fig. 3-1) – the former are ascribed to mat formation which either trapped grains horizontally, or rotated them to that orientation during mat-decomposition and compaction, while the latter laminae reflect short-lived depositional events (Noffke et al., 1997a). No examples

have yet been identified from the rock record, and such features are problematic to differentiate from non-biogenic compaction-related grain fabrics. Other fabrics indicating evidence for microbial mats can include **lamina-specific mineral enrichment**, in either heavy minerals ('d', Fig. 3-1) (Gerdes et al., 2000a) or micas (Garlick, 1981, 1988).

Positive bed-top features resulting from mat growth are relatively common and display a wide range of morphologies and sizes, varying from **tufts, pinnacles and pustules** ('f' in Fig. 3-1), to **bulges** and **reticulate ornamentation** (cf. 'elephant skin'; Gehling, 1999; 'g' in Fig. 3-1); a range of **wrinkle structures** ('h', Fig. 3-1; Hagadorn and Bottjer, 1997, 1999; Schieber, 1998a, 1999; see also Chapter 6(a)) may also result. **Dome-like features** ('e', Fig. 3-1; see also 'sand stromatolites' in Figs. 4(a)-11 to -13) are reported from several Precambrian and younger sandstone occurrences (Davis, 1968; Garlick, 1981, 1988; Schieber, 1998a). They are ascribed to higher levels of wave or current energy (which favour more rapid syndepositional lithification), with **planar forms** resulting from lower energy levels (Hoffman, 1976; Sami and James, 1993).

Mat growth can be disturbed by currents, winds, the development of gas, or by intermittent desiccation. These processes lead to buckling, doming and rupturing of microbially bound surficial sand layers. Modern examples (Reineck et al., 1990; Gerdes et al., 1993) and ancient analogues (Gehling, 1999) of these antiformal structures are termed **petees**. Within this framework, and depending on intensity of the disruption to mat-bound sand layers, either more simple networks or more complex sinuous **petee ridges** may result, the latter commonly encompassing rupture of the microbial surfaces (respectively, 'i' and 'j' in Fig. 3-1).

Features formed due to metabolic effects of growing mat (see Chapter 4(b))

In modern mats, metabolic processes like photosynthesis have been observed to shift carbonate solubility enough to cause precipitation of carbonate minerals between and along filaments within the growing mats (Krumbein, 1974, 1986; Gerdes and Krumbein, 1987; Chafetz and Buczynski, 1992; Chafetz, 1994). These **mineral precipitation effects** can be preserved within the rock record as: irregular ooids (Gerdes and Krumbein, 1987), disseminated carbonate grains (e.g., Kropp et al., 1997), micritic cement between terrigenous grains, and highly lamina-specific carbonate cementation within laminated sandstones. Another metabolic effect would be the formation of **very early diagenetic dolomite** (Gebelein and Hoffman, 1973) from high Mg concentrations in sheaths of living filamentous cyanobacteria. If mat-internal carbonate precipitation is voluminous enough, detrital grains of quartz and mica may be encased in a carbonate matrix and form '**floating grains**' upon lithification. In ancient examples, a '**coated grain**' fabric denotes sand- and silt-sized grains that are surrounded by fine-grained sericitic material (Bouougri and Porada, 2002; Draganits and Noffke, 2004). Modern analogues have been described by various authors (e.g., Gerdes et al., 2000a; Noffke et al., 2001a, 2003b). Coated grain fabrics have been related to the presence of intergranular coccoidal bacteria and their mucilages (e.g., Noffke et al., 2001a). Clays transported through the grain fabric by uprising or circulating groundwater are trapped on grain surfaces by mucilage coatings

and may later form sericite. Alternatively, biogeochemical processes within the microbial mat itself (Krumbein and Werner, 1983) may allow clay accumulation.

Forming in inherently permeable sandstones, syngenetic signatures, such as lamina-specific carbonate cementation, are easily overprinted by subsequent diagenetic processes. Certain textural features, however, like **'floating' terrigenous grains** in a carbonate matrix, suggest precompactional and possibly syngenetic carbonate formation (Garlick, 1988; Schieber, 1998). In addition, highly **lamina-conformable distribution of pyrite** may reflect the metabolic activity of sulphate-reducing bacteria beneath the photosynthetic surface layer of a mat (Schieber, 1989a).

Features formed by physical mat destruction (see Chapter 4(c))

Physical destruction of microbially bound sediments generates a wide range of sedimentary features that may occur at the original mat location, or may be observed in redeposited materials. Because physically deposited sand layers are grain-supported, they can not shrink upon desiccation. Thus, if sand layers are found to contain shrinkage cracks, an additional component that shrinks upon desiccation must originally have been present between the sand grains. Clays, for example, can function in this role. Yet, because the resulting rock could readily be identified as a clay-rich sandstone, contraction upon desiccation would be expected. In the absence of a clay matrix, however, a water-rich matrix of microbial filaments and extracellular polymer substance (EPS) would be the most likely cause for shrinkage upon desiccation. The resulting **sand crack patterns** vary from incomplete networks to polygonal patterns, and may even form complexly superimposed sets of spindle-shaped cracks (Bouougri and Porada, 2002; Schieber, 2004; Sarkar et al., 2004, 2006) that can themselves become filled with sand (e.g., 'k', Fig. 3-1).

In this book, the spectrum of shrinkage-related features is expanded by adding features observed at crack margins in modern sandy mats, such as **curled crack margins, overgrown, and upturned crack margins** (see Chapter 4(c)). The latter have not yet been described explicitly from ancient sandy mat deposits.

Sinuuous to circular sand cracks restricted to ripple troughs form a special case, known as **'Manchuriophycus'** ('l' in Fig. 3-1), probably formed due to thickened mat layers within ripple troughs (Pflüger, 1999; Gehling, 2000). Microbial mats may also maintain a measure of cohesiveness for some time after burial. Deformation of such microbially-bound sand layers may result in contrasting behaviour to over- and underlying layers of loose, non-bound sand. **Non-penetrative microfaults** ('m', Fig. 3-1) in sandstones have been interpreted to reflect cohesive behaviour of buried mat layers in sandy deposits (Pflüger, 1999; Gehling, 1999).

Binding of sand surfaces by microbial mats significantly enhances their resistance to erosion (e.g., Neumann et al., 1970), but erosion, tearing, and transport of mat fragments will commence once strong currents are active. Erosion of mat-bound sands leads to sedimentary features that are distinctively different from those that form during the

erosion and reworking of a loose and unbound sand substrate. Whereas in the latter case we can expect to see scouring and the formation of wave and current ripples over wide expanses of the sand bed, mat erosion tends to produce localized erosional ‘windows’ where the protective mat is removed. These exposed areas can then be remoulded into a rippled surface by wave and current action, forming **rippled patches** in an otherwise smooth sandy surface (‘n’, Fig. 3-1). This feature is known from both modern tidal flats (Reineck, 1979; Gerdes et al., 1985b), and the rock record (McKenzie, 1972; Reineck, 1979; Schieber, 1998a). It is important to note that a smooth transition results between purported mat surface and rippled sandstones in these features (see also Chapter 7(i)).

The inherent cohesiveness of mat-bound sand surfaces also leads to the formation of **flipped-over edges** (‘o’ in Fig. 3-1) of partially eroded mat surfaces, as well as to the redeposition of deformed and **rolled-up mat fragments**, also called ‘roll-ups’ (‘p’ and ‘w’, Fig. 3-1). Modern examples are reported by Reineck (1979) and Gerdes et al. (2000a), and inferred ancient equivalents by Schieber (1998a, 1999), Garlick (1981, 1988), Simonson and Carney (1999), and Eriksson et al. (2000). A subclass of the eroded mat fragments is comprised by **microbial sand chips** (Pflüger and Gresse, 1996; Bouougri and Porada, 2002; Sarkar et al., 2006; ‘q’ in Fig. 3-1). These probably reflect a longer transport history than roll-ups, resulting in a measure of sorting and abrasion. What sets microbial sand chips apart from irregular and rolled-up mat fragments are their typically smaller dimensions (a few centimetres at most), similar sizes within a given occurrence, plastic deformation, and commonly observed current-alignment (Pflüger and Gresse, 1996). In places they may even show imbrication (Bouougri and Porada, 2002).

Desiccation of microbially-bound sand surfaces results in many instances in polygonal crack patterns (see above) and a surface that is covered by rigid, **curved sand chips** (several centimetres across; ‘v’, Fig. 3-1). Upon erosion, the latter can be transported as intraclasts and become incorporated into high energy sandstone deposits. Fossil examples are reported by Garlick (1988) and Schieber (1998a). In the absence of textural differences (grain size, lamination), these sand chips may be difficult to distinguish from their sandstone matrix. In that case diagenetic effects, such as mat decay mineralization related to the organic content of the chips (Garlick, 1988; Schieber, 1999), may be the only means for their recognition in the rock record (see below also).

Features resulting from mat decay and diagenesis (see Chapter 4(b) and (d))

Once mat decay begins, decay gases can disturb the sediment beneath the mats as well as disrupting the mats themselves, forming **gas domes**, **convoluted internal lamination** (‘r’, Fig. 3-1) (Gerdes et al., 2000a), and **ruptured gas domes** known as ‘*Astropolithon*’ (Pflüger, 1999; ‘s’, Fig. 3-1). The substrate cohesiveness implicit in the radial ruptures of ‘*Astropolithon*’ domes also provides a supporting argument for the former presence of a mat. Gas development related to mat decay also helps form the more severely disturbed and ruptured **petee** structures (‘j’ in Fig. 3-1). The steep slopes of the troughs and the flat tops associated with ‘*Kinneyia*’ **style ripples** (‘t’ in Fig. 3-1) led Pflüger (1999) to propose that these formed due to gas trapping beneath a mat. However, ‘*Kinneyia*’ can

easily be confused with wrinkled mat surfaces ('g' and 'h', Fig 3-1) (see also, Chapter 6(a)), and many '*Kinneyia*' described in the literature rather resemble the round-crested microbial wrinkle marks described by Hagadorn and Bottjer (1999).

The permeability of sand results in rapid microbial metabolization of buried organic matter. This circumstance largely obviates survival of organic matter as an indicator of microbial mats in sandstones. However, mats constitute sharply defined geochemical boundaries (Bauld, 1981), and anaerobic decay beneath them favours formation of 'anoxic' minerals such as pyrite, siderite, and ferroan dolomite. These authigenic minerals can locally cement the sand, occlude porosity, and result in '**mat-decay mineralization**' (Schieber, 1998a). The 'ghosts' of filaments may be preserved in these cements. Preservation of thin, stratiform horizons of mat decay minerals ('u', Fig. 3-1) in shallow water sandstones suggests the former presence of microbial mats (Gerdes et al., 1985b; Garlick, 1988). Different minerals are favoured depending whether water chemistry is marine or fresh (e.g., respectively, pyrite versus siderite). The burial of rigid ('v', Fig. 3-1) or soft fragments ('q' and 'w', Fig. 3-1) of re-sedimented mat can induce similar cementation once decay sets in and can preserve a ghost outline of the transported mat fragments (Garlick, 1988; Pflüger and Gresse, 1996; Schieber, 1998a).

Microbial mat features preserved in shales (see Chapter 5)

Figure 3-2 summarises features that have been observed in shales that were subject to microbial mat influences during deposition or diagenesis. Genetic processes inferred to be responsible for these biogenic sedimentary structures are shown on a clockwise-arranged continuum, from mat growth to final destruction and diagenesis (cf. Schieber, 2004).

Features formed as a result of mat growth

Because of the high degree of compaction that surface muds are subjected to upon burial, surface features formed due to binding, trapping, and baffling by microbial mats on muddy substrates is preserved as a much more subtly defined surface relief in the rock record (Schieber, 2004). Despite this, **wavy-crinkly laminae** ('a' in Fig. 3-2) form, that are distinctively different from the parallel laminae that form in mudstones from suspension settling during physical sedimentation processes (Schieber, 1986; Fairchild and Herrington, 1989; O'Brien, 1990; Goth, 1990; Wuttke and Radtke, 1993; Goth and Schiller, 1994). Colonisation of irregular sediment surfaces (such as an intraclast conglomerate) by mats can result in **bed-smoothing** ('b', Fig. 3-2). In non-mat mudstones, compactional effects above comparable relief are generally detectable for a greater distance upward from the underlying surface irregularities. Differences in the **behaviour** of shales under conditions of **soft sediment loading** (Schieber, 1986) also provides evidence for bed-surface stabilization by a mat cover. As an example, where silt layers have been deposited on mat-bound mudstone surfaces, only minor load features result ('d', Fig. 3-2), whereas miniature ball-and-pillow structures tend to form on non-mat mudstones ('c', Fig. 3-2).

In: *Atlas of microbial mat features preserved within the clastic rock record*, Schieber, J., Bose, P.K., Eriksson, P.G., Banerjee, S., Sarkar, S., Altermann, W., and Catuneau, O., (Eds.)J. Schieber et al. (Eds.), Elsevier, p. 39-52. (2007)

In contrast to the wavy-crinkly carbonaceous laminae discussed above, which are reported mainly from inferred subtidal and shelf settings (Schieber, 1986; Fairchild and Herrington, 1989; Logan et al., 1999a), **domal buildups** of variable amplitude and spacing have been observed in nearshore mudstones ('e' and 'f', Fig. 3-2; Schieber, 1998a). The inherent rapid weathering of mudstones has likely hampered recognition and preservation of a variety of other, similar occurrences in the rock record.

Event sedimentation such as caused by floods and storms, will bury growing mats under a sudden influx of sediment, thereby causing interruption of mat growth. Such intermittent events can then lead to '**striped shales**' with alternating mat and event layers ('g', Fig. 3-2; Schieber, 1986; Logan et al., 1999a; see Chapter 7(b) and (c)). As mat cover expands over a muddy substrate, intermittent deposition of thin clay drapes can lead to a feature called **false cross-lamination** ('h', Fig. 3-2) at the edge of the expanding mat patches. This feature reflects the rapid re-establishment of mats (via vertical movement of buried filaments) on top of the recently deposited clay drapes, followed by their lateral expansion (Schieber, 1986).

Although fossil **petee structures** formed on muddy substrates have not yet been identified in the rock record, petee formation is independent of substrate calibre (e.g., Reineck et al., 1990; Gerdes et al., 2000a). Analogous structures, at a smaller scale, are known in modern mud puddles.

Lamina-specific grain selection, as evinced by mat laminae enriched in mica flakes ('i' in Fig. 3-2) has been observed in mud-based microbial mats (Schieber, 1998a). As for their sandy microbial mat equivalents, the underlying causes for this type of grain enrichment are not well understood (Gerdes et al., 2000a).

Features formed as a consequence of mat metabolism

Syngenetic carbonate precipitation can be associated with mats growing on a muddy substrate, as analogously found for sandy sediments above (Schieber, 2004). Such syngenetic carbonate deposition is for example suggested by **randomly oriented mica flakes** in conformable carbonate-rich laminae (Schieber, 1998a) or by **terrigenous grains floating in a carbonate matrix**. In the first case, partial rotation of the flakes to more horizontal orientations may occur during cementation later in the burial history, as compaction begins to play a role. Examples from the rock record are illustrated in Chapter 7(b).

Where **bituminous substances** can still be extracted from suspected fossil mat deposits, determination of carbon isotopes, biomarkers, and sulphur isotopes, can suggest likely metabolic pathways operating at the time of deposition (Brassell, 1992; Logan et al., 1999a). Such **biomarkers** may help to indicate which bacteria dominated in the living mats, such as cyanobacteria (oxygenic photosynthesis), photosynthetic sulphur bacteria

(anaerobic photosynthesis), or sulphide-oxidising bacteria (chemoautotrophy) (Gallardo, 1977; Williams and Reimers, 1983).

Features produced by physical mat destruction

In general, features resulting from erosion of mat-bound muddy surfaces have close analogues in those formed by erosion of microbially-bound sandy sediments. Mat-bound mud layers display ‘within layer’ cohesiveness when eroded and transported (‘l’ in Fig. 3-2) as well as a different rheological quality (firm-doughy, less compactible) when compared to ‘normal’ mud layers (which are soft-fluid- and yoghurt-like; ‘k’ in Fig. 3-2) (Schieber, 1986). **Flipped-over mat edges** (‘j’ in Fig. 3-2), **overfolded mat layers** (‘k’, Fig. 3-2), and variably-sized **‘roll-up’ structures** are all known from ancient mudstone examples (Schieber, 1986, 1998a, 1999). **Torn mats and mat fragments** commonly display frayed edges (‘m’, Fig. 3-2), sometimes called the ‘blotting paper effect’ in modern mats (Gerdes et al., 1993). This feature is also found in ancient examples (Schieber, 1999).

Analogous to sandy mat deposits, desiccation and shrinkage of muddy microbial mats produces cracks and dried out mat chips. Yet, because muddy substrates would, due to their water content, show these features anyway, the discrimination of palaeo-desiccation features in suspected muddy mat deposits (such as cracks and dried-out mat chips) remains problematic. In modern muddy settings, mats will cause modifications of crack morphology and crack-edges (Gerdes et al., 1993); however, comparable features from the rock record have not yet been reported.

Desiccation of thin biofilms on mudflats causes cracking and curling upon drying, and these paper-thin fragments can then be transported by either water (Fagerstrom, 1967) or wind (Trusheim, 1936). Being desiccated, they resist compaction when re-deposited and can then produce **irregular impressions** if they come to rest on a semi-dried muddy surface of stiff consistency (‘n’, Fig. 3-2). An ancient example has been described by Horodyski (1982, 1983).

Dried-out mat fragments may also float, and can then carry detrital nearshore grains to deeper parts of a water body (Fagerstrom, 1967). Such rafting processes are inferred for **clusters of coarser grains** (‘o’, Fig. 3-2) found in otherwise ‘pure’ mudstones (Olsen et al., 1978; Schieber, 1999). In Phanerozoic-age sedimentary rocks, analogous raft deposition may occur through floating plant debris or animal carcasses, as well as by fecal pellets. Thus, distinguishing coarse grain-clusters due to the latter processes from those formed through mat-rafting is very difficult in Phanerozoic mudrocks (Schieber, 2004).

Features formed under conditions of mat decay and diagenesis

Gas formation in submerged mats, due to either photosynthesis or decay processes, may cause rupturing and detachment of mat fragments that can then float to the surface (Fagerstrom, 1967). Any attached coarse grains can then be rafted offshore, forming

coarse-grain-clusters in a mudstone matrix upon deposition (Schieber, 2004) ('o', Fig. 3-2). This feature is analogous to that described immediately above, and highlights the polygenetic nature of many mat-related sedimentary structures.

When anaerobic decay of organic matter occurs beneath a growing mat, favourable conditions occur for **precipitation of 'anoxic' minerals like pyrite, siderite, and ferroan dolomite**. Within marine settings, hydrogen sulphide commonly forms beneath the mat, and pyrite will crystallise (Berner, 1984). Depending on the amount of iron available in the environment, manifestations in the rock record may range from **carbonaceous laminae dusted with tiny pyrite grains** to **strongly pyritic laminae** ('p', Fig. 3-2) that essentially mimic the wavy-crinkly mat lamination ('a' in Fig. 3-2; Schieber, 1989a; see also Chapter 7(b) and (e)). During early diagenesis, pyrite overgrowth and cementation of the original fine-grained pyrite may occur (Strauss and Schieber, 1990; Chapter 7(b)). Analogous **recrystallization and enlargement of carbonate minerals** takes place in layers with syngenetic carbonate accumulations ('q', Fig. 3-2). As further burial leads to maturation of organic matter and reduction of organic content (hydrocarbon formation), biomarkers and kerogens are gradually destroyed. However, the low inherent permeability of mudstones prevents complete organic matter destruction (in contrast to most permeable sandstones) and **anastomosing carbonaceous laminae** may be preserved ('r', Fig. 3-2) (Schieber, 2004).

Complex structures

Because of its all-embracing nature, the organizational scheme presented by Schieber (2004) is used to order the manifold structures illustrated in this book in a process-response context. Not all mat-related structures observable in modern environments are explicitly included in this scheme, in part due to their lacking descriptions and due to a lack of ancient equivalents. A variety of 'complex structures' are briefly introduced to complement the range of features summarized in Figs. 3-1 and 3-2.

As stated in the introduction, the structures and features in this atlas are considered sedimentary structures that can be used as tools for unravelling depositional palaeoenvironments, analogous to their physical sedimentary counterparts. However, even features due to physical forces on mat-bound sedimentary surfaces cannot always be subsumed under the rules of sedimentation formulated by Stokes' Law (Krumbein and Schellnhuber, 1990). Observations of modern microbial mats in stressed environments (e.g., intertidal and supratidal flats of arid coasts) have shown that physical damage to surfaces overgrown by mats immediately prompts complex physiological strategies of the community members to again find their most optimal ecological niches after the disturbance has passed.

Observation of a 'living' mat surface also provides insight into the history of the mat which often undergoes changes within hours. Many structures are not simple results of 'events', but rather reflect a series of reactions of the microbiota to 'events', even more so as combinations of different life styles are involved rather than only one. Each

variation of irradiation, each rain drop, each grain of sediment deposited on the surface is an ‘event’ triggering a reaction. All these ‘events’ are a source for energy input into the system. It’s not necessary to think only of ‘catastrophic events’ like sudden burial, flooding and destruction etc. Synergistic reactions of the system, possibly in a kind of feedback, are able to produce meso-/macroscopic structures. This could also explain why many structures are so similar in appearance and may thus be classified, e.g., as ‘bulges’, ‘petees’ etc (see Chapter 6(c)). The effect of a cause may not be uniform across the area occupied by a mat. Mat destruction and mat growth may occur directly adjacent to each other.

Zavarzin (2003) stated that cyanobacteria-dominated mats are a highly sustainable biotic system that dominated Earth from the early Proterozoic to the end of the Neoproterozoic, and still survive in habitats where successor organisms (seaweeds etc.) and metazoans are excluded. To understand such spatial and temporal sustainability of mats in spite of often unpredictable disturbances by physical processes (e.g., cracking, tearing, transport, scouring), the approach of ‘parahistology’ seems to be particularly important. In terms of structure, cohesion, and distribution of tasks of individual cells, biofilms and microbial mats are compared to tissues (Krumbein et al., 2003) which are similar to cells of living plants or to animal tissues, and which start immediately with protective actions against injuries. Some patterns of self-healing are illustrated in Figures 3-3A and -3B (see also mat growth concurrent with desiccation and cracking in Chapter 4(f)). Another aspect to understand is why these systems flourish particularly well in intertidal and supratidal flats of arid coasts in spite of an immense physical stress, due to the cooperative growth of different morphological and metabolic types in well-protected biofilms and microbial mats (Wachendörfer et al., 1994; Costerton and Stoodley, 2003).

Patterns of self-healing, the successful protection of biofilm organisms against water-loss and UV irradiation, or the textural and geometric similarity of mats in spite of the diversity of habitats (Zavarzin, 2003) cannot be explained by linear processes. As Krumbein and Schellnhuber (1990, 1992) stated, the processes apparently are not thermodynamic but follow laws governing dissipative or dynamic systems. These are attributes of complex structures resulting from self-organised processes, controlled by ‘complex fractal system physics’ (Krumbein and Schellnhuber, 1990).

Features observed in complex structures

Figures 3-3 to 3-5 illustrate examples of complex structures that reflect growth responses of mats that were triggered by external forces. All these structures cannot be linearly classified according to physical deformation or destruction, but rather indicate concomitant vital dynamics and ‘parahistology’ attributes of biofilms and microbial mats following nonlinear laws in their growth and extension behaviour.

Under thin water cover (a few centimetres), small surface elevations such as ripple crests, PS (photosynthetic) domes (Chapter 6(c)) or gas domes may become sites of localised microbial growth of filamentous cyanobacteria, e.g., *Lyngbya* sp. (Fig. 3-3A to -3D). In

such cases, growth patterns may deviate from the normally reticulate arrangement of crests (see Fig. 3-3A).

On sand deposited by wind or currents and concomitantly agglutinated and stabilised by coccoidal biofilms (e.g., *Synechococcus* sp.), photosynthetic (PS) domes resulting from metabolic processes of the filamentous mat below are overgrown, thus expanding the biofilm substrates (Fig. 3-4A). The processes are combined when induced growth on ripple crests leads to development of coalescing PS domes which in turn are overgrown (Fig. 3-4B). Growth and expansion of biofilm substrates (see also Fig. 3-4C - 4H) is stimulated by physical factors, such as slight topographic elevations.

Striking complex structures can, for example, result from a succession starting with the production of gas bubbles, their trapping and stabilisation by EPS, and microbial overgrowth using the interfaces of bubbles. Bursting of these bubbles produces characteristic lizard-skin textures (Fig. 3-4G). These, as well as the overgrown and stabilised rims of burst bubbles (Fig. 3-4H), may become preserved and appear as more or less distinct microstructures on ancient bedding surfaces.

Shrinkage cracks developed in microbial mats after extended subaerial exposure may become sites of localised 'induced growth' (see definition of terms in Chapter 6(c)), because of uprising water due to hydraulic 'upward pressure' in the sedimentary mat substratum. The emerging groundwater which in sabkhas is often well enriched in dissolved inorganic nutrients, e.g., phosphates (Javor, 1989), offers a liquid medium for biofilms/microbial layers to grow and expand within the cracks and may produce flat (Fig. 3-5A) or bulge-like expansion structures (Fig. 3-5B) completely spanning the cracks.

Upon subaerial exposure, small elevated areas on the surface of thin mats may become sites of accelerated desiccation, shrinkage and initial cracking at the crests or peaks (Fig. 3-5C). If the desiccating mat still possesses sufficient elasticity, involution or 'curling' of the crack margins may occur (Fig. 3-5D). If hydraulic 'upward pressure' in the mat substratum is still sufficient to cause ascent of groundwater, the 'curled margins' may be overgrown and preserved as linear, bulge-like features on the mat surface (Fig. 3-5E). Cracking starting at the peaks of domal features in a thin mat frequently leads to circular/subcircular 'curled margin' structures (Fig. 3-5F). These may also be overgrown by further microbial expansion.

Impressive examples of the intimate interplay of physical processes and vital dynamics in thick biolaminates, modern and ancient, are seen in Figures 4(f)-1 and -2. These 'complex structures' reflect incremental upturning of a crack margin and microbial growth during repeated tidal cycles with periods of subaerial exposure and inundation, respectively.

Conclusions

As with most scientific fields, the various classification schemes proposed for microbial mats in terrigenous clastic sediments have advantages and disadvantages when applied to specific case studies, and it can seldom be argued that one scheme is intrinsically superior. In Chapter 2 of this book, Gerdes points out that microbial growth-related structures (in Schieber's 2004 organizational scheme) can easily be related to the five processes implicit in the MISS scheme of Noffke et al. (2001a), namely biostabilisation, levelling, baffling-trapping-binding, imprinting, and microbial grain separation. Analogously, she notes that the mat metabolism-, mat destruction- and mat decay-related structure groupings of Schieber (2004) also relate to biostabilisation. While in many ways, the differences between the various classification schemes discussed may hinge on semantics, the scheme that proves to be most practical in everyday application and is most widely adopted will eventually prevail. It is also likely that the best aspects of each scheme will ultimately be combined into a standard classification as research proceeds. The history of sandstone classifications in sedimentary petrology provides an example how this may play out eventually.

Other, less well-known classification schemes make use of physical properties of preserved mat-induced features in clastic sedimentary rocks (e.g., Sarkar et al., 2004). Due to its combination of simplicity and inclusion of a wide range of interacting genetic factors, we have elected to adopt the Schieber (2004) scheme in this book. This decision is not meant to detract from other classification systems.

References

- Awramik, S.M., 1984. Ancient stromatolites and microbial mats. In: Cohen, Y., Castenholz, R.W., Halvorson, H.O. (Eds.), *Microbial Mats: Stromatolites*. Alan R. Liss, New York, pp. 1-22.
- Altermann, W., 2004. Evolution of life and Precambrian bio-geology. In: Eriksson, P.G., Altermann, W., Nelson, D.R., Mueller, W.U., Catuneanu, O. (Eds.), *The Precambrian Earth: Tempos and Events*. *Developments in Precambrian Geology* 12, Elsevier, Amsterdam, pp. 587-591.
- Bauld, J., 1981. Geobiological role of cyanobacterial mats in sedimentary environments: production and preservation of organic matter. *BMR J. Australian Geol. Geophys.* 6: 307-317.
- Berner, R.A., 1984. Sedimentary pyrite formation: an update. *Geochim. et Cosmochim. Acta* 48: 605-615.
- Bouougri, E., Porada, H., 2002. Mat-related sedimentary structures in Neoproterozoic peritidal passive margin deposits of the West African Craton (Anti-Atlas, Morocco). *Sediment. Geol.* 153: 85-106.
- Brassell, S.C., 1992. Biomarkers in sediments, sedimentary rocks and petroleum: biological origins, geological fate and applications. In: Pratt, L.M., Comer, J.B., Brassell, S.C. (Eds.), *Geochemistry of Organic Matters in Sediments and Sedimentary Rocks*. Soc. Econ. Paleontol. Mineral. Short Course 27, Tulsa, Oklahoma, pp. 29-72.
- Chafetz, H.S., 1994. Bacterially induced precipitates of calcium carbonate and lithification in microbial mats. In: Krumbein, W.E., Paterson, D.M., Stal, L.J. (Eds.), *Biostabilization of Sediments*. Bibliotheks- und Informationssystem der Carl von Ossietzky Universität Oldenburg, (BIS)-Verlag, Oldenburg, pp. 149-164.
- Chafetz, H.S., Buczynski, C., 1992. Bacterially induced lithification of microbial mats. *Palaios* 7: 277-293.
- Costerton, J., Stoodley, P., 2003. Microbial biofilms: protective niches in ancient and modern geomicrobiology. In: Krumbein, W.E., Paterson, D.M., Zavarzin, G.A. (Eds.), *Fossil and Recent Biofilms* (Preface). Kluwer Academic Publishers, Dordrecht, pp. xv-xxi.
- Davis, R.A., 1968. Algal stromatolites composed of quartz sandstone. *J. Sediment. Petrol.* 38: 953-955.
- Draganits, E., Noffke, N., 2004. Siliciclastic, domed stromatolites from the Lower Devonian Muth Formation, NW Himalaya. *J. Sediment. Res.* 74: 191-202.
- In: *Atlas of microbial mat features preserved within the clastic rock record*, Schieber, J., Bose, P.K., Eriksson, P.G., Banerjee, S., Sarkar, S., Altermann, W., and Catuneanu, O., (Eds.) J. Schieber et al. (Eds.), Elsevier, p. 39-52. (2007)

- Eriksson, P.G., Simpson, E.L., Eriksson, K.A., Bumby, A.J., Steyn, G.L., Sarkar, S., 2000. Muddy roll-up structures in siliciclastic interdune beds of the c. 1.8 Ga Waterberg Group, South Africa. *Palaios* 15:177-183.
- Fagerstrom, J.A., 1967. Development, flotation and transportation of mud crusts-neglected factors in sedimentology. *J. Sediment. Petrol.* 37: 73-79.
- Fairchild, I.J., Herrington, P.M., 1989. A tempestite-stromatolite-evaporite association (late Vendian, East Greenland): a shoreface-lagoon model. *Precambrian Res.* 43: 101-127.
- Gallardo, V.A., 1977. Large benthic microbial communities in sulfide biota under Peru-Chile subsurface counter current. *Nature* 268: 331-332.
- Garlick, W.G., 1981. Sabkhas, slumping, and compaction at Mufulira, Zambia. *Econ. Geol.* 76: 1817-1847.
- Garlick, W.G., 1988. Algal mats, load structures, and syndimentary sulfides in Revett Quartzites of Montana and Idaho. *Econ. Geol.* 83: 1259-1278.
- Gebelein, C.D., Hoffman, P., 1973. Algal origin of dolomite laminations in stromatolitic limestone. *J. Sediment. Petrol.* 43: 603-613.
- Gehling, J.G., 1999. Microbial mats in terminal Proterozoic siliciclastics: Ediacaran death masks. *Palaios* 14: 40-57.
- Gehling, J.G., 2000. Environmental interpretation and a sequence stratigraphic framework for the terminal Proterozoic Ediacara Member within the Rawnsley Quartzite, south Australia. *Precambrian Res.* 100: 65-95.
- Gerdes, G., Krumbein, W.E., 1987. *Biolaminated Deposits. Lecture Notes in Earth Sciences* 9. Springer-Verlag, Berlin, 183 pp.
- Gerdes, G., Krumbein, W.E., Reineck, H.-E., 1985b. The depositional record of sandy, versicolored tidal flats (Mellum Island, southern North Sea). *J. Sediment. Petrol.* 55: 265-278.
- Gerdes, G., Claes, M., Dunajtschik-Piewak, K., Riege, H., Krumbein, W.E., Reineck, H.-E., 1993. Contribution of microbial mats to sedimentary surface structures. *Facies* 29: 61-74.
- Gerdes, G., Klenke, T., Noffke, N., 2000a. Microbial signatures in peritidal siliciclastic sediments: a catalogue. *Sedimentology* 47: 279-308.
- In: *Atlas of microbial mat features preserved within the clastic rock record*, Schieber, J., Bose, P.K., Eriksson, P.G., Banerjee, S., Sarkar, S., Altermann, W., and Catuneau, O., (Eds.) J. Schieber et al. (Eds.), Elsevier, p. 39-52. (2007)

Goth, K., 1990. Der Messeler Ölschiefer- ein Algenlaminit. Courier Forschungsinstitut Senckenberg. 131, pp. 1-143.

Goth, K., Schiller, W., 1994. Miozäne Algenlaminite von Hausen in der Rhön. Palaeontologische Zeitschrift 68: 287-297.

Hagadorn, J.W., Bottjer, D.J., 1997. Wrinkle structures: microbially mediated sedimentary structures common in subtidal siliciclastic settings at the Proterozoic-Phanerozoic transition. Geology 25: 1047-1050.

Hagadorn, J.W., Bottjer, D.J., 1999. Restriction of a Late Neoproterozoic biotope: suspect-microbial structures and trace fossils at the Vendian-Cambrian transition. Palaios 14: 73-85.

Hagadorn, J.W., Pflüger, F., Bottjer, D.J., 1999. Unexplored microbial worlds. Palaios 14: 1-2.

Hofmann, H.J., 1973. Stromatolites: characteristics and utility. Earth-Sci. Rev. 9: 339-373.

Hoffman, P.F., 1976. Stromatolite morphogenesis in Shark Bay, western Australia. In: Walter, M.R. (Ed.), Stromatolite. Developments in Sedimentology 20, Elsevier, Amsterdam, pp. 261-271.

Hofmann, H.J., 2000. Archean stromatolites as microbial archives. In: Riding, R.E., Awramik, S.M. (Eds.), Microbial Sediments. Springer-Verlag, Berlin, pp. 315-327.

Horodyski, R.J., 1982. Impressions of algal mats from the Middle Proterozoic Belt Supergroup, northwestern Montana. Sedimentology 29: 285-289.

Horodyski, R.J., 1983. Paleontology of Proterozoic shales and mudstones: examples from the Belt Supergroup, Chuar Group and Pahrump Group, western USA. Precambrian Res. 61: 241-278.

Javor, B., 1989. Hypersaline Environments – Microbiology and Biogeochemistry. Springer-Verlag, Berlin, 328 pp.

Kropp, J., Block, A., Von Bloh, W., Klenke, T., Schellnhuber, H.J., 1997. Multifractal characterization of microbially induced magnesian calcite formation in recent tidal flat sediments. Sediment. Geol. 109: 37-51

Krumbein, W.E., 1974. On precipitation of aragonite on the surface of marine bacteria. Naturwissenschaften 61: 167.

In: *Atlas of microbial mat features preserved within the clastic rock record*, Schieber, J., Bose, P.K., Eriksson, P.G., Banerjee, S., Sarkar, S., Altermann, W., and Catuneau, O., (Eds.)J. Schieber et al. (Eds.), Elsevier, p. 39-52. (2007)

- Krumbein, W.E., 1986. Biotransfer of minerals by microbes and microbial mats. In: Leadbeater, B.S.C., Riding, R. (Eds.), *Biominalization in Lower Plants and Animals*. Proc. Systematics Assoc. Symposium, Univ. Birmingham, April, 1985, Oxford University press, Oxford, pp. 55-72.
- Krumbein, W.E., Schellnhuber, H.J., 1990. Geophysiology of carbonates as a function of bioplanets. In: Itteccot, V.S. (Ed.), *Facets of Modern Biogeochemistry*. Springer-Verlag, Berlin, pp. 5-22.
- Krumbein, W.E., Schellnhuber, H.J., 1992. Geophysiology of mineral deposits – a model for a biological driving force of global changes through earth history. *Terra Nova* 4: 351-362.
- Krumbein, W.E., Werner, D., 1983. The microbial silica cycle. In: Krumbein, W.E. (Ed.), *Microbial Geochemistry*. Blackwell Science, Oxford, pp. 125-157.
- Krumbein, W.E., Brehm, U., Gerdes, G., Gorbushina, A.A., Levit, G., Palinska, K.A., 2003. Biofilm, biodictyon, biomat microbialite, oolites, stromatolites-geophysiology, global mechanisms and parahistology. In: Krumbein, W.E., Paterson, D.M., Zavarzin, G.A. (Eds.), *Fossil and Recent Biofilms*. Kluwer Academic Publishers, Dordrecht, pp. 1-28.
- Logan, G.A., Calver, C.R., Gorjan, P., Summons, R.E., Hayes, J.M., Walter, M.R., 1999a. Terminal Proterozoic mid-shelf benthic microbial mats in the Centralian Superbasin and their environmental significance. *Geochim. et Cosmochim. Acta* 63: 1345-1358.
- McKenzie, D.B., 1972. Tidal sand flat deposits in Lower Cretaceous Dakota Group near Denver, Colorado. *The Mountain Geol.* 9: 269-277.
- Neumann, A.C., Gebelein, C.D., Scoffin, T.P., 1970. The composition, structure and erodability of subtidal mats, Abaco, Bahamas. *J. Sediment. Petrol.* 40: 274-297.
- Noffke, N., 1998a. Multidirected ripple marks rising from biological and sedimentological processes in modern lower supratidal deposits (Mellum Island, southern North Sea). *Geology* 26: 879-882.
- Noffke, N., Gerdes, G., Klenke, T., Krumbein, W.E., 1997a. A microscopic sedimentary succession indicating the presence of microbial mats in siliciclastic tidal flats. *Sediment. Geol.* 110: 1-6.
- Noffke, N., Gerdes, G., Klenke, T., Krumbein, W.E., 2001a. Microbially induced sedimentary structures - a new category within the classification of primary sedimentary structures. *J. Sediment. Res.* A71: 649-656.
- In: *Atlas of microbial mat features preserved within the clastic rock record*, Schieber, J., Bose, P.K., Eriksson, P.G., Banerjee, S., Sarkar, S., Altermann, W., and Catuneau, O., (Eds.) J. Schieber et al. (Eds.), Elsevier, p. 39-52. (2007)

Noffke, N., Gerdes, G., Klenke, T., 2003b. Benthic cyanobacteria and their influence on the sedimentary dynamics of peritidal depositional systems (siliciclastic, evaporitic salty, and evaporitic carbonatic). *Earth-Sci. Rev.* 62: 163-176.

O'Brien, N.R., 1990. Significance of lamination in the Toarcian (Lower Jurassic) shales from Yorkshire, Great Britain. *Sediment. Geol.* 67: 25-34.

Olsen, P.E., Remington, C.L., Corliss, B., Thompson, K.S., 1978. Change in Late Triassic lacustrine communities. *Science* 201: 729-733.

Pettijohn, F.J., Potter, P.E., 1964. *Atlas and Glossary of Primary Sedimentary Structures*. Springer-Verlag, Berlin, 370 pp.

Pflüger, F., 1999. Matground structures and redox facies. *Palaios* 14: 25-39.

Pflüger, F., Gresse, P.G., 1996. Microbial sand chips- a non-actualistic sedimentary structure. *Sediment. Geol.* 102: 263-274.

Reineck, H.-E., 1979. Rezente und fossile Algenmatten und Wurzelhorizonte. *Natur und Museum* 109: 290-296.

Reineck, H.-E., Gerdes, G., Claes, M., Dunajtschik, K., Riege, H., Krumbein, W.E., 1990. Microbial modification of sedimentary surface structures. In: Heling, D., Rothe, P., Förstner, U., Stoffers, P. (Eds.), *Sediments and Environmental Geochemistry*. Springer-Verlag, Berlin, pp. 254-276.

Sami, T.T., James, N.P., 1993. Evolution of an early Paleozoic foreland basin carbonate platform, lower Pethei Group, Great Slave Lake, north-west Canada. *Sedimentology* 40: 403-430.

Sarkar, S., Banerjee, S., Eriksson, P.G., 2004. Microbial mat features in sandstones illustrated. In: Eriksson, P.G., Altermann, W., Nelson, D.R., Mueller, W.U., Catuneanu, O. (Eds.), *The Precambrian Earth: Tempos and Events*. *Developments in Precambrian Geology* 12, Elsevier, Amsterdam, pp. 673-675.

Sarkar, S., Banerjee, S., Samanta, P., Jeevankumar, S., 2006. Microbial mat-induced sedimentary structures in siliciclastic sediments: examples from the 1.6 Ga Chorhat Sandstone, Vindhyan Supergroup, M.P., India. *J. Earth Sys. Sci.* 115: 49-60.

Schieber, J., 1986. The possible role of benthic microbial mats during the formation of carbonaceous shales in shallow Mid-Proterozoic basins. *Sedimentology* 33: 521-536.

Schieber, J., 1998a. Possible indicators of microbial mat deposits in shales and sandstones: examples from the Mid-Proterozoic Belt Supergroup, Montana, USA. *Sediment. Geol.* 120: 105-124.

In: *Atlas of microbial mat features preserved within the clastic rock record*, Schieber, J., Bose, P.K., Eriksson, P.G., Banerjee, S., Sarkar, S., Altermann, W., and Catuneanu, O., (Eds.) J. Schieber et al. (Eds.), Elsevier, p. 39-52. (2007)

Schieber, J., 1999. Microbial mats in terrigenous clastics: the challenge of identification in the rock record. *Palaios* 14: 3-12.

Schieber, J., 2004. Microbial mats in the siliciclastic rock record: a summary of the diagnostic features. In: Eriksson, P.G., Altermann, W., Nelson, D.R., Mueller, W.U., Catuneanu, O. (Eds.), *The Precambrian Earth: Tempos and Events. Developments in Precambrian Geology* 12, Elsevier, Amsterdam, pp. 663-673.

Simonson, B.M., Carney, K.E., 1999. Roll-up structures: evidence of *in situ* microbial mats in Late Archean deep shelf environments. *Palaios* 14: 13-24.

Trusheim, F., 1936. Wattenpapier. *Natur und Volk* 66: 103-106.

Wachendörfer, V., Krumbein, W.E., Schellnhuber, H.J., 1994. Bacteriogenic porosity of marine sediments – a case of biomorphogenesis of sedimentary rocks. In: Krumbein, W.E., Paterson, D.M., Stal, L.J. (Eds.), *Biostabilization of Sediments. Bibliotheks- und Informationssystem der Carl von Ossietzky Universität Oldenburg, (BIS)-Verlag, Oldenburg*, pp. 203-220.

Walter, M.R. (Ed.), 1976. *Stromatolites. Developments in Sedimentology* 20, Elsevier, Amsterdam, 790 pp..

Walter, M.R., Bauld, J., Des Marais, D.J., Schopf, J.W., 1992. A general comparison of microbial mats and microbial stromatolites: bridging the gap between the modern and the fossil. In: Schopf, J.W., Klein C. (Eds.), *The Proterozoic Biosphere: An Interdisciplinary Study*. Cambridge University Press, New York, pp. 335-338.

Williams, L.A., Reimers, C., 1983. Role of bacterial mats in oxygen-deficient marine basins and coastal upwelling regimes: preliminary report. *Geology* 11: 267-269.

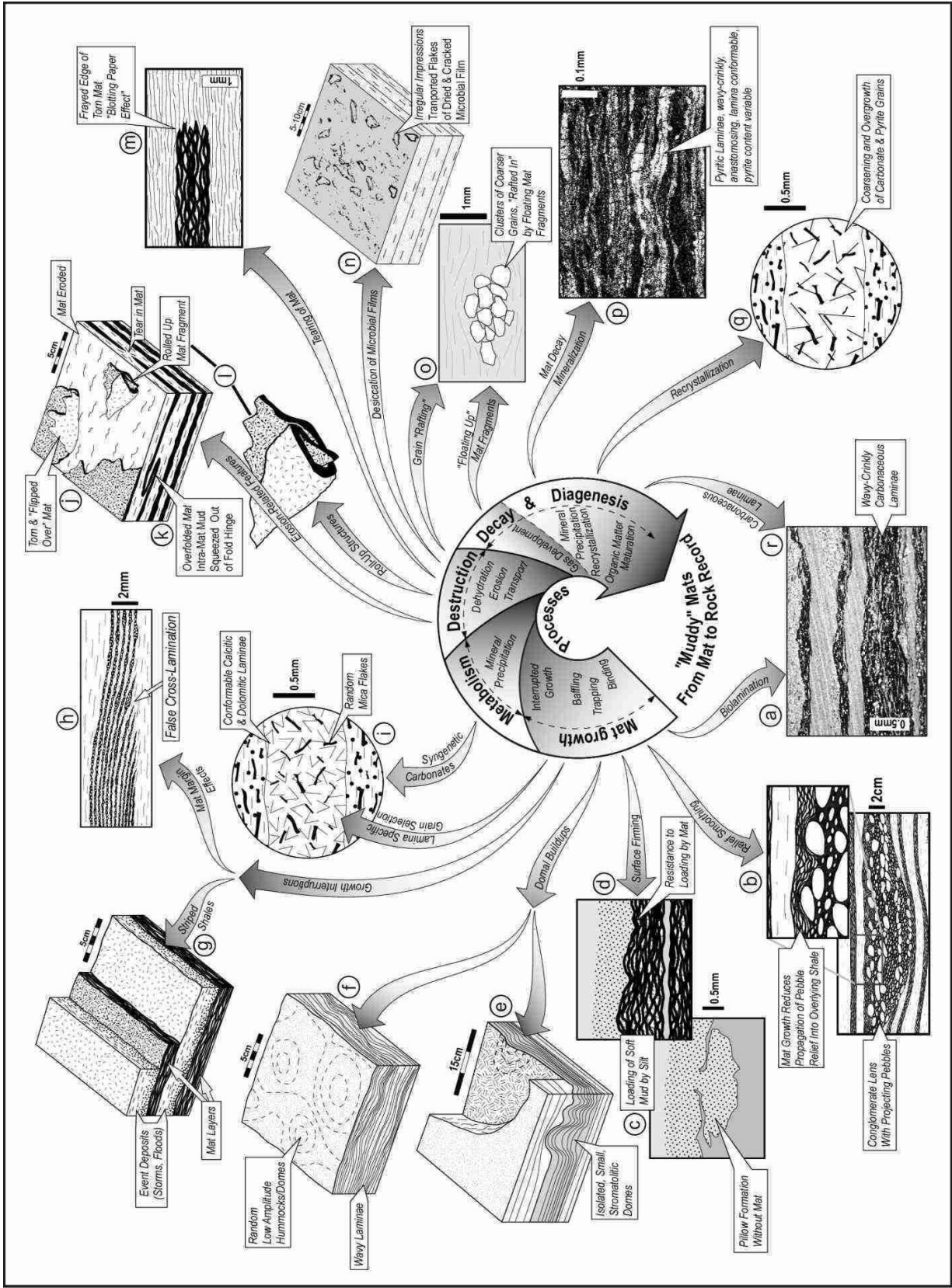
Wuttke, M., Radtke, G., 1993. Agglutinierende Mikrobenmatten im Profundal des mitteleozänen Eckfelder Maar-Sees bei Manderscheid/Eifel (Bundesrepublik Deutschland). -*Mainzer Naturwissenschaftliches Archiv* 31: 115-126.

Zavarzin, G.A., 2003. Diversity of cyano-bacterial mats. In: Krumbein, W.E., Paterson, D.M., Zavarzin, G.A. (Eds.), *Fossil and Recent Biofilms*. Kluwer Academic Publishers, Dordrecht, pp. 141-150.

In: *Atlas of microbial mat features preserved within the clastic rock record*, Schieber, J., Bose, P.K., Eriksson, P.G., Banerjee, S., Sarkar, S., Altermann, W., and Catuneanu, O., (Eds.)J. Schieber et al. (Eds.), Elsevier, p. 39-52. (2007)

Fig. 3-1: Features found in sandstones where microbial mats flourished in the past:

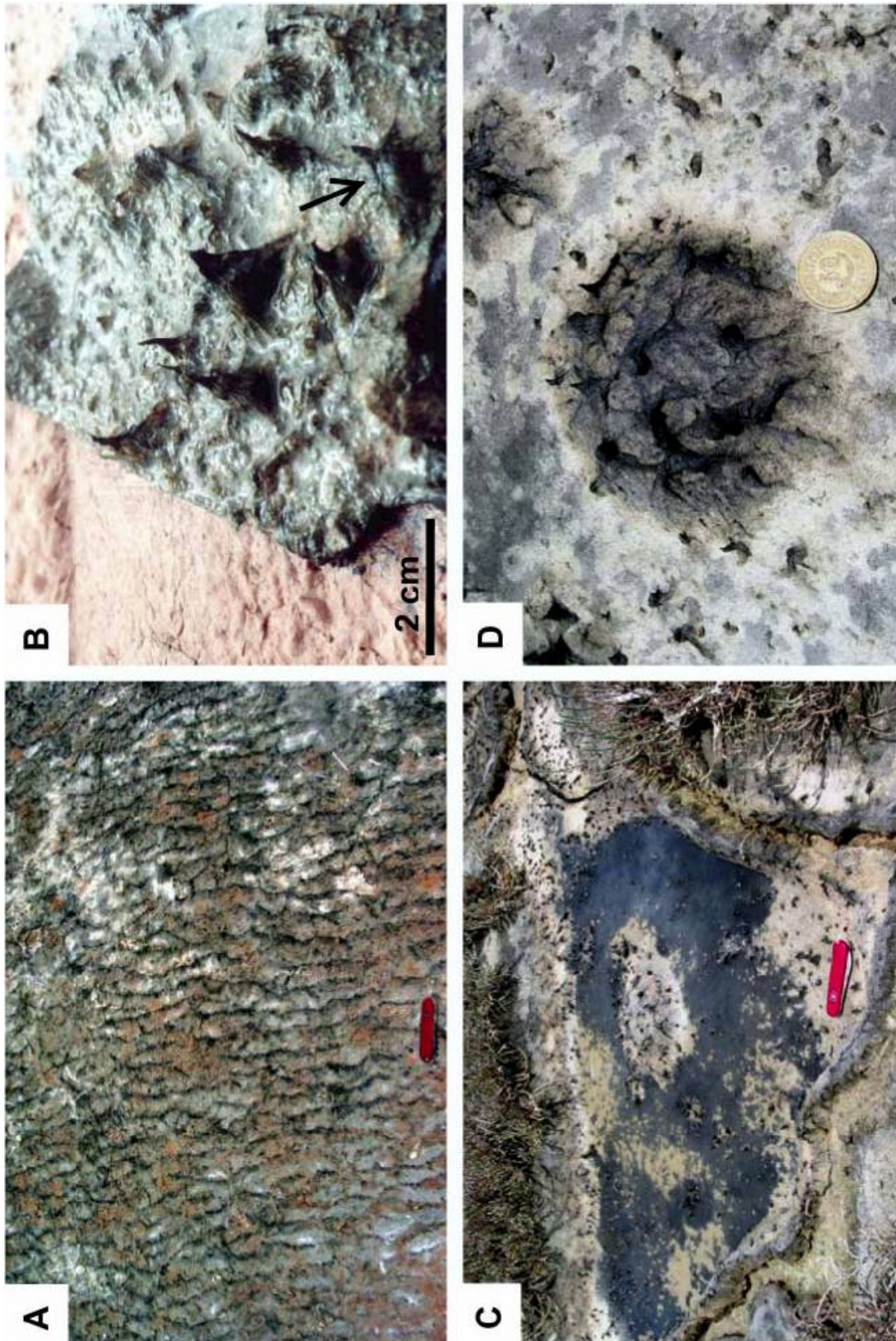
Genetic processes are arranged clockwise along a continuum from active growth of mats to final destruction during diagenesis. Modified after Schieber (2004; his figure 7.9-1).



In: *Atlas of microbial mat features preserved within the clastic rock record*, Schieber, J., Bose, P.K., Eriksson, P.G., Banerjee, S., Sarkar, S., Altermann, W., and Catuneau, O., (Eds.) J. Schieber et al. (Eds.), Elsevier, p. 39-52. (2007)

Fig. 3-2: Features found in mudstones where microbial mats flourished in the past:

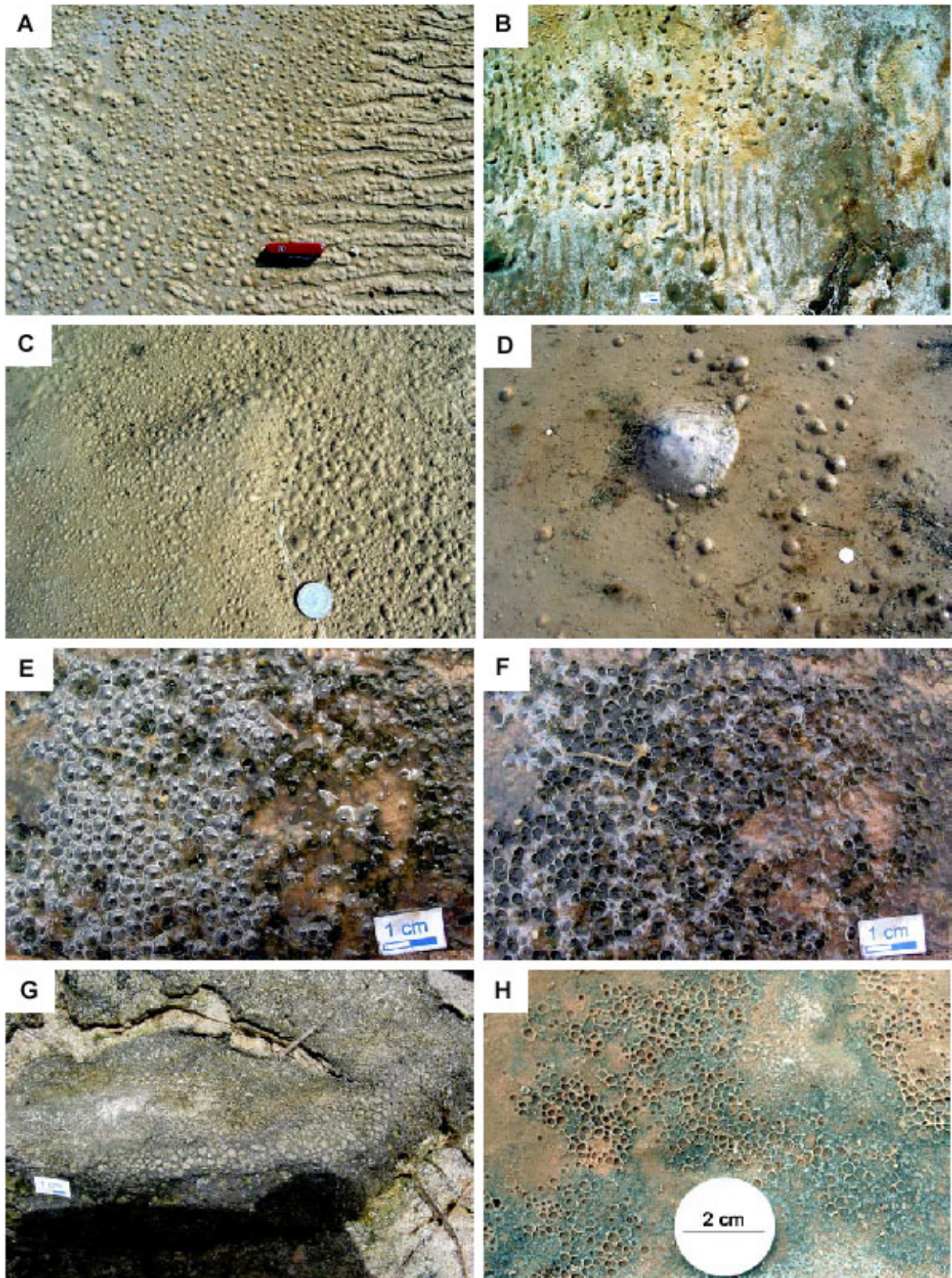
Genetic processes are arranged clockwise along a continuum from active growth of mats to final destruction during diagenesis. Modified after Schieber (2004; his figure 7.9-2).



In: *Atlas of microbial mat features preserved within the clastic rock record*, Schieber, J., Bose, P.K., Eriksson, P.G., Banerjee, S., Sarkar, S., Altermann, W., and Catuneau, O., (Eds.) J. Schieber et al. (Eds.), Elsevier, p. 39-52. (2007)

Fig. 3-3: Structures resulting from ‘induced growth’ at small topographic elevations on mat surfaces:

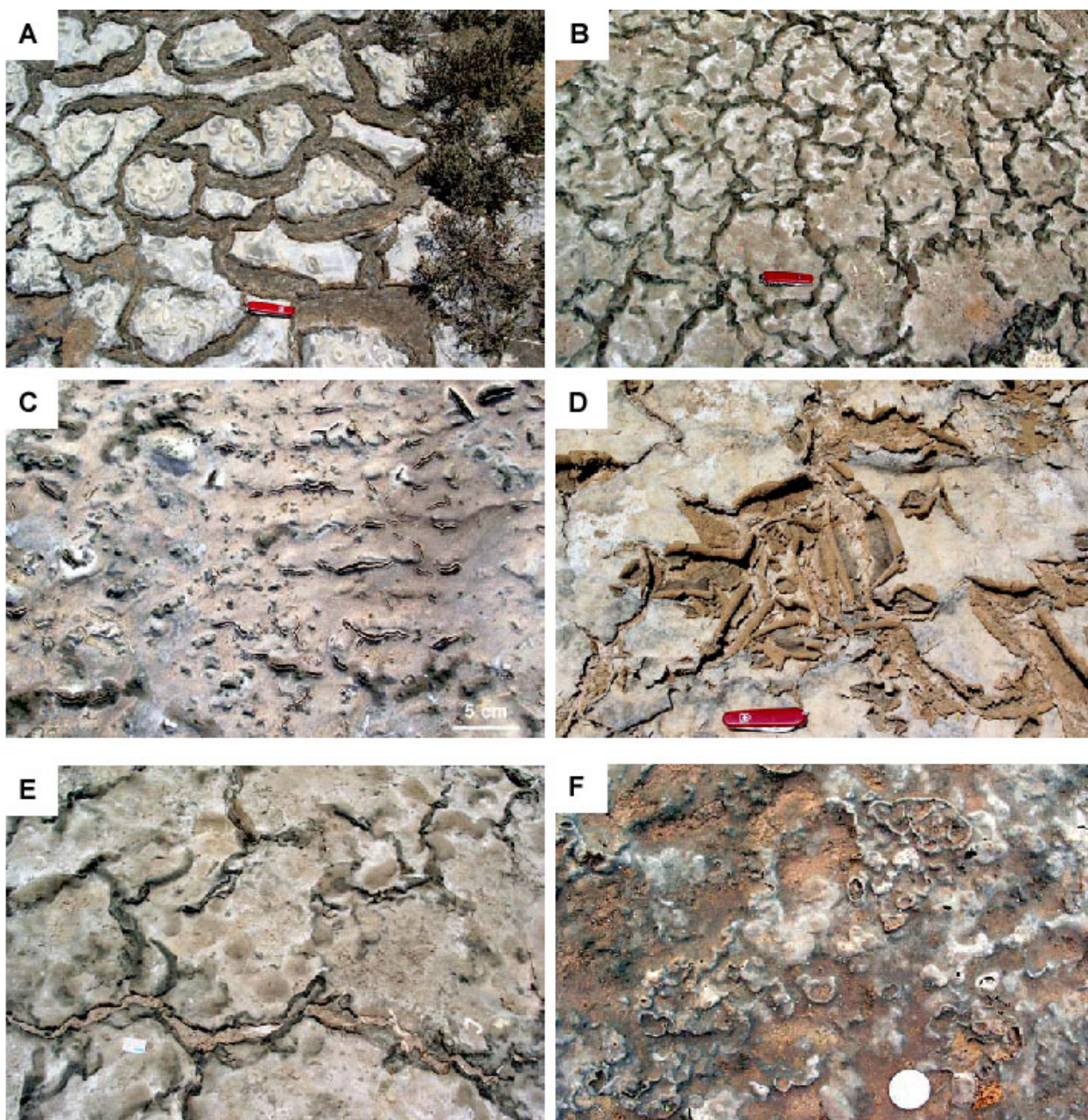
(A) Selective growth of filamentous cyanobacteria (*Lyngbya* sp.) along small-scale current ripple crests after temporary marine inundation. Lower supratidal zone, Bhar Alouane, southern Tunisia. Scale (knife) is 8 cm. (B) Shows a piece of a mat cut from the surface of a living mat for photographic documentation. Filamentous cyanobacteria (*Lyngbya* sp.) form isolated tufts upon photosynthetic domes (PS domes – see Chapter (c)). Note partly exposed PS dome (black arrow) at tuft close to lower image border. The black *Lyngbya* filaments were carefully removed with a knife to expose the milky-white membrane consisting of coccoid cyanobacteria and strongly cohesive EPS material comprising the upper surface of the PS dome. Upper intertidal zone, Bou Ghrara, southern Tunisia. (C) Supratidal puddle partly filled with sulphide-rich water, and with central gas dome, formed by trapped uprising gas from decaying mats. Note isolated *Lyngbya* tufts on gas dome and along elevated margins of puddle. Lower supratidal zone, Bhar Alouane, southern Tunisia. Scale (knife) is 8 cm. (D) Gas dome in dried-up portion of lower supratidal puddle, with reticulate growth pattern and tufts produced by *Lyngbya* sp. The structure may be interpreted as an ‘escape structure’ documenting escape of motile cyanobacteria from hostile, sulphide-rich water in the puddle. It should be noted that, for varying day/night conditions within an active mat community, many photosynthetic cyanobacteria can tolerate reducing and sulphidic conditions; however, in this case, the sulphide-rich water provides permanent reducing and sulphidic conditions. Supratidal zone, Bhar Alouane, southern Tunisia. Scale (coin) is 25 mm. All photos: Hubertus Porada.



In: *Atlas of microbial mat features preserved within the clastic rock record*, Schieber, J., Bose, P.K., Eriksson, P.G., Banerjee, S., Sarkar, S., Altermann, W., and Catuneau, O., (Eds.) J. Schieber et al. (Eds.), Elsevier, p. 39-52. (2007)

Fig. 3-4: Structures reflecting ‘induced growth’ related to photosynthetic bubbles and PS domes:

(A) Congregation of overgrown PS-domes in flat area of a shallow depression (left side), reflecting prolonged microbial activity of coccoidal cyanobacteria under a thin cover of residual water. Note isolated PS domes on ripple crests (right side) produced at higher water levels in the depression. Scale (knife) is 8 cm. Supratidal zone, Bhar Alouane, southern Tunisia. (B) Stabilised and overgrown small-scale current ripples; ripple crests partly associated with isolated PS domes and small elongate bulges, resulting from coalescence of domes. Ripple crests were preferred sites of microbial activity and localised accretion of biomass. Scale is 2 cm. Supratidal zone, Bhar Alouane, southern Tunisia. (C) Sediment surface with overgrown PS domes of various sizes in relation to microtopographic features. Large PS domes indicate prolonged activity of coccoidal cyanobacteria under thin cover of residual water in microtopographic lows. Scale (coin) is 25 mm. Supratidal zone, Bhar Alouane, southern Tunisia. (D) Isolated PS domes on fresh flat mat of mainly coccoidal cyanobacteria. The domes are stabilised by EPS and partly overgrown. Note large gas dome, about 10 cm in diameter and stabilised by EPS, in centre of photo. The large gas dome likely originated from uprising gases of buried, decaying mats. Scale (coin) is 25 mm. Shallow supratidal pond, Bhar Alouane, southern Tunisia. (E) View of active microbial community and freshly produced photosynthetic bubbles. The bubbles are stabilised by EPS and may merge to form larger units. Lower supratidal puddle, Bhar Alouane, southern Tunisia. (F) Same surface as in Fig. 3-4E, after artificial destruction of gas bubbles. Note EPS formerly stabilising bubbles, now forming light, circular, nutrient-rich rims, and interstitial patches around dark hollows. Lower supratidal puddle, Bhar Alouane, southern Tunisia. (G) ‘Lizard-skin’ texture on microbial mat surface, reflecting structures left behind after bursting of photosynthetic gas bubbles. The microbial mat, developed along the margin of a supratidal puddle, has developed a bulge-like termination towards the puddle. Note shrinkage crack with upturned and slightly curled margins. Scale is 1 cm. Lower supratidal puddle, Bhar Alouane, southern Tunisia. (H) Circular to hexagonal pattern, possibly resulting from burst photosynthetic gas bubbles; partly overgrown and almost disappearing (left side). Rims may have been sites of first overgrowth or internal growth, using nutrient-rich EPS that once stabilised the bubbles. Margin of supratidal pond, El Gourine, southern Tunisia. All photos: Hubertus Porada.



In: *Atlas of microbial mat features preserved within the clastic rock record*, Schieber, J., Bose, P.K., Eriksson, P.G., Banerjee, S., Sarkar, S., Altermann, W., and Catuneau, O., (Eds.) J. Schieber et al. (Eds.), Elsevier, p. 39-52. (2007)

Fig. 3-5: Structures reflecting ‘induced growth’ related to mat shrinkage and cracking:

(A) Network of wide shrinkage cracks developed in microbial mat after prolonged subaerial exposure. Crack margins are upturned and locally curled. Crack openings and margins are overgrown by new, flat biofilm/mat layers, microbial growth being induced by ascending groundwater due to hydraulic “upward pressure” in the sedimentary mat substratum. Scale (knife) is 8 cm. Upper intertidal zone, El Jellabia; southern Tunisia.

(B) Polygonal network of narrow shrinkage cracks in mature microbial mat. Cracks are overgrown by bulge-like mat expansion structures resulting from localised excessive microbial growth and biomass accretion, induced by uprising groundwater in the crack openings. Scale (knife) is 8 cm. Lower supratidal zone, Bhar Alouane, southern Tunisia.

(C) Thin microbial mat with small linear shrinkage cracks located preferably along crests of overgrown ripples, initial cracking being induced by more advanced desiccation and shrinkage on small microtopographic elevations. Note dark zones in lower and upper left part of photo, representing sites of uprising groundwater and induced microbial activity. Supratidal zone, Bhar Alouane, southern Tunisia.

(D) Thin microbial mat with wide, irregular shrinkage cracks and curled crack margins. Involution or ‘curling’ of crack margins may occur if a ‘contractional force’ emanates from the shrinking but still elastic surface layer, involving adhering mat layers below. Scale (knife) is 8 cm. Supratidal zone, El Gourine, southern Tunisia.

(E) Thin microbial mat exhibiting various generations of cracking and microbial overgrowth. First generation, narrow shrinkage cracks in upper and left part of photo are overgrown by bulging mat expansion structures; second generation, wider cracks in central part of photo have developed curled margins and are overgrown by flat mat layers; a youngest, third generation crack in the lower part of the photo partly follows 2nd generation cracks, rupturing flat mat layers and inheriting overgrown crack margins. Scale is 2 cm. Supratidal zone, Bhar Alouane, southern Tunisia.

(F) Thin microbial mat of mainly coccoid cyanobacteria, with numerous domal features on the surface. Initial cracking at peaks of domal features frequently leads to circular/subcircular ‘curled margin’ structures which subsequently may be overgrown. Scale (coin) is 25 mm. Supratidal zone, El Gourine, southern Tunisia. All photos: Hubertus Porada.